AGU100 ADVANCING EARTH AND SPACE SCIENCE

Geochemistry, Geophysics, Geosystems

RESEARCH ARTICLE
10.1029/2017GC006969

Special Section:
Clumped Isotope Geochemistry: From Theory to Applications

Assessment of Factors Controlling Clumped Isotopes and $\delta^{18}O$ Values of Hydrothermal Vent Calcites

Tobias Kluge[1,2,3], Cédric M. John[3], Ronny Boch[4], and Sándor Kele[5]

[1]Institute of Environmental Physics, Heidelberg University, Heidelberg, Germany, [2]Heidelberg Graduate School of Fundamental Physics, Heidelberg University, Heidelberg, Germany, [3]Department of Earth Science and Engineering and Qatar Carbonate and Carbon Storage Research Centre, Imperial College London, London, UK, [4]Institute of Applied Geosciences, Graz University of Technology, Graz, Austria, [5]Institute for Geological and Geochemical Research, Hungarian Academy of Sciences, Budapest, Hungary

Key Points:
- Fast-growing hydrothermal vent calcites tend toward a small (~0.01‰) effect of DIC speciation on clumped isotope Δ_{47} at the studied pH 6–8
- $\delta^{18}O$ offsets of up to −2‰ of samples rapidly grown at pH 6–8 are consistent with expectations related to growth kinetics
- Fast isotopic equilibration of DIC at lower pH and elevated water temperature could explain the absence of further disequilibrium offsets

Supporting Information:
- Supporting Information S1

Correspondence to:
T. Kluge,
tobias.kluge@iup.uni-heidelberg.de

Citation:
Kluge, T., John, C. M., Boch, R., & Kele, S. (2018). Assessment of factors controlling clumped isotopes and $\delta^{18}O$ values of hydrothermal vent calcites. *Geochemistry, Geophysics, Geosystems*, *19*, 1844–1858. https://doi.org/10.1029/2017GC006969

Received 13 APR 2017
Accepted 17 APR 2018
Accepted article online 27 APR 2018
Published online 30 JUN 2018

Abstract The clumped isotope composition of $CaCO_3$ (Δ_{47}) is a geochemical proxy that can provide mineral formation temperatures and, together with measured carbonate $\delta^{18}O$, inferred fluid $\delta^{18}O$ values. Under natural conditions, carbonates form within a relatively wide pH range and varying growth rates which are typically not reflected in laboratory-based calibrations (mostly ~pH 8, moderate growth rates). A pH and growth-rate dependence is known for oxygen isotopes and was also postulated for clumped isotopes. Theoretical predictions suggest that Δ_{47} values could lie between the carbonate equilibrium value and the value inherited from the dissolved inorganic carbon (predicted offset: +0.04‰ pH < 4 and −0.025‰ at high pH > 12). Here we test whether pH (in addition to temperature) is recorded in the carbonate clumped isotope composition using modern calcites from natural travertine-forming streams and scales precipitated in pipes of deep geothermal wells from Italy, Hungary, and Turkey (pH: 6.1–7.5, T: 33–100°C). Although a comparison of all samples with expected equilibrium values in this pH range and known formation temperatures reveals only an insignificant Δ_{47} offset (0.006 ± 0.004‰, 1SE, $n = 9$), the clumped isotope values of samples with the highest growth rates (0.014 ± 0.007‰, 1SE, $n = 5$) are consistent with the theoretical prediction attributable to pH of 0.01‰. Similarly, deviations in $\delta^{18}O$ of up to −2‰ follow a growth-rate dependence. This field-based study shows that pH-related effects are mostly small for Δ_{47} in the subsurface environment at lower pH and that high mineral growth rates control the magnitude of this disequilibrium.

1. Introduction

Carbonate clumped isotopes constitute a highly successful tool for geothermometry that is applied to an increasing number of research questions in Earth sciences (e.g., Eiler, 2011). Carbonate clumped isotopes are a specific subgroup of multiply substituted isotopologues (Eiler, 2013) and refer to carbonate molecules that show a "clumping" of two rare isotopes in one molecule. The abundance of multiply substituted isotopologues is governed by thermodynamic parameters for a system at internal isotopic equilibrium (Wang et al., 2004) and can be calculated using partition functions that depend on the rotational and vibrational frequencies of the relevant bonds. For CO_2 gas produced from acid digestion of carbonates, the abundance of ^{13}C–^{18}O bonds carries information about the carbonate precipitation temperature (e.g., Ghosh et al., 2006; Guo et al., 2009; Schauble et al., 2006) and is expressed as difference from the stochastic distribution (Δ_{47} value; Affek & Eiler, 2006; Eiler & Schauble, 2004):

$$\Delta_{47} = \left[\left(\frac{R^{47}}{R^{47*}} - 1\right) - \left(\frac{R^{46}}{R^{46*}} - 1\right) - \left(\frac{R^{45}}{R^{45*}} - 1\right)\right]$$

*terms refer to the stochastic ratio, numerator terms to the measured ratios

The Δ_{47}-T relationship was calculated for CO_2 gas via an evaluation of the isotope exchange reactions (Wang et al., 2004) and for carbonates using first principle lattice dynamics (Schauble et al., 2006). The Δ_{47}-T relationship was assessed using inorganic carbonates from laboratory precipitates (e.g., Defliese et al., 2015; Dennis & Schrag, 2010; Ghosh et al., 2006; Kelson et al., 2017; Kluge et al., 2015; Zaarur et al., 2013) and natural travertine samples (Kele et al., 2015) that show a relationship of increasing Δ_{47} values with decreasing

temperature. Many biogenic carbonates also follow these inorganic calibrations (e.g., Affek, 2012; Bonifacie et al., 2017; Grauel et al., 2013). These calibrations provide a basis for paleoclimate studies using a diverse range of natural carbonate samples (e.g., Affek, 2012; Eiler, 2011) and more generally for reconstructing the thermal history of minerals and fluids (Huntington & Lechler, 2015).

For the currently used laboratory-based calibrations (Defliese et al., 2015; Dennis & Schrag, 2010; Ghosh et al., 2006; Kelson et al., 2017; Kluge et al., 2015; Zaarur et al., 2013), carbonates were mostly precipitated at relatively low ionic strength (few tens of mmol/L; mainly from dissolving $CaCO_3$) and near neutral pH conditions (pH $\sim$ 8). For example, for the initially used Δ_{47}-T calibration of Ghosh et al. (2006) carbonates were precipitated in the laboratory at a pH value of $\sim$8 following a method similar to that of Kim and O'Neil (1997) where HCO_3^- is the main dissolved inorganic carbonate (DIC) species (>90%; e.g., Mook, 2000). In contrast, at low pH (pH $<$ 6) H_2CO_3 and dissolved CO_2 are the dominating DIC species, and at pH >10.3 CO_3^{2-} is the main species. Although the neutral pH conditions in the experiments of Ghosh et al. (2006), Dennis and Schrag (2010), Zaarur et al. (2013), and Kluge et al. (2015) cover a large portion of conditions typically prevailing during natural carbonate precipitation it leaves the question of a potential influence of fluid compositions deviating from laboratory conditions on the ^{13}C–^{18}O clumping untouched. Kelson et al. (2017) studied a wider range of solution pH values (5–10) and found no significant effect on Δ_{47} values for typical experimental growth rates (0.4–800 mg/d per Erlenmeyer flask, assuming a surface area of the beaker of 0.02 m^2 this corresponds to 3 $\times$ 10^{-3}–4 μmol/(m^2s)), generally consistent with theoretical work of Watkins and Hunt (2015). However, Watkins and Hunt (2015) also indicate that higher growth rates (>10 μmol/(m^2s)) at pH 7 may yield measurable deviations of about 0.01‰ for Δ_{47}. In contrast, at pH 10 Watkins and Hunt (2015) predict a DIC Δ_{63} value independent of growth rate. In case of travertines and hydrothermal scales vertical growth rates of 1–10 mm/yr are typically observed (e.g., Boch et al., 2016), which is above the typical experimental range, approaches the kinetic growth limit (e.g., Watkins & Hunt, 2015) and is therefore well-suited to test a potential pH influence. Further evidence for the necessary high growth rate comes from instantaneous carbonate formation that confirmed an isotopic influence of the DIC-speciation effect at higher pH values of 7.5–12 (Tripati et al., 2015). Still, an assessment of a potential pH effect at lower pH and high mineral formation rates is lacking.

A pH-related speciation effect is well known for oxygen isotopes and can be substantial (up to 20‰; e.g., Beck et al., 2005; Dietzel et al., 2009; Rollion-Bard et al., 2003; Usdowski et al., 1991; Zeebe, 1999; Zeebe & Wolf-Gladrow, 2001). Between pH 4 and 10, the mean DIC $\delta^{18}O$ decreases by about 1.6‰ per pH unit (at 19°C; Zeebe, 1999). At pH 7–8 and high growth rates, Watkins and Hunt (2015) predict changes in carbonate $\delta^{18}O$ of up to -2‰ relative to the equilibrium calcite composition. For clumped isotopes, it was initially estimated to be small and potentially negligible ($\sim$0.02‰; Guo et al., 2008). Hill et al. (2012, 2014) theoretically derived the clumped isotope composition of each DIC species. The clumped isotope composition of the DIC pool is the weighted sum of all DIC components and therefore varies with pH. Hill et al. (2012, 2014) found slightly larger maximum effects on the order of 0.04‰ that are significant relative to the achievable analytical precision of $\sim$0.01‰. The Δ_{47} value of carbonates may inherit the isotopic composition of the DIC pool. Carbonate that forms rapidly by dehydration of HCO_3^- is expected to be $\sim$0.03‰ higher in the clumped isotope composition than by direct precipitation from CO_3^{2-}, and $\sim$0.03‰ lower than during formation following the conversion of H_2CO_3 (Hill et al., 2014). The predicted deviation of equilibrium calcite is $\sim$0.01‰ at pH 4–9 and $-$0.025‰ at pH 12–14 (Hill et al., 2014). Given this speciation effect is captured in the carbonate mineral, it can impact on temperatures derived from the Δ_{47}-T calibration that is based on carbonates precipitated from a HCO_3^- dominated solution at a pH value of $\sim$8. High growth rates, however, are necessary for the pH effect to be recorded in the precipitating carbonate as rapid growth would prevent isotopic equilibration between DIC and water and amongst the DIC species (e.g., Kele et al., 2011; Tripati et al., 2015).

In natural systems significant deviations from a HCO_3^- dominated solution (pH $\sim$8) can frequently occur. pH values above 8.5 were observed, for example, in the extracellular calcifying fluid of marine organisms such as corals and foraminifera (Al-Horani et al., 2003; Cohen & McConnaughey, 2003; de Nooijer et al., 2009; Venn et al., 2011). In natural as well as anthropogenically affected alkaline aqueous solutions even much higher pH values were measured (pH > 11.5; e.g., Andrews et al., 1997; Boch et al., 2015; Chavagnac et al., 2013; Clark et al., 1992; Falk et al., 2016). pH and the related speciation of the dissolved inorganic carbon in the calcifying fluid during biomineralization has been suggested to potentially influence the carbonate Δ_{47}

values in various studies (e.g., Eagle et al., 2013; Grauel et al., 2013; Henkes et al., 2013). However, this could not be confirmed empirically so far. Eagle et al. (2013) investigated the pH effect on cultured molluscs, but found no systematic influence on the Δ_{47} values in the pH range of 7.5–8.0. Similarly, Thiagarajan et al. (2011) and Tripati et al. (2010) did not observe deviations of the Δ_{47} value from the expected value in deep-sea corals and foraminifera, respectively. Fast-growing hermatypic corals (calcification rate of 5–6 μmol/(m^{2}s)) exhibit deviations from equilibrium Δ_{47} values, however, the related Δ_{47}-δ^{18}O relationship does not agree with a pH-associated mechanism (Saenger et al., 2012). Observations from travertines, pool carbonates, and tufa material of various locations did not yield a significant trend of Δ_{47} with pH (Kele et al., 2015). Inorganic carbonates between pH 5 and 10 in the experiments of Kelson et al. (2017) showed no pH effect, potentially due to not sufficiently high growth rates ($\leq$4 μmol/(m^{2}s)). In contrast, Guo et al. (2012) and Tripati et al. (2015) precipitated barium carbonates almost instantaneously at different pH values and obtained Δ_{47} values that differed from carbonates precipitated from HCO_3^- dominated solutions at the same temperature. For example, the instantaneously precipitated witherite at pH 7.8–12 in the experiments of Tripati et al. (2015) revealed a very strong pH effect related to the DIC speciation. Deviations from equilibrium calcite Δ_{47} values were about $+0.015‰$ for HCO_3^- and $-0.05‰$ for CO_3^{2-}, close to the predictions of Hill et al. (2014).

Direct empirical or experimental observations of the DIC speciation at lower pH $<$ 7 and at high growth rates are missing. Low pH values $<$7 are observed in (mostly CO_2-rich) subsurface fluids linked to hydrothermal activity (Kele et al., 2015) or diagenesis (Hesse, 1987; Gilfillan et al., 2009; Kharaka & Hanor, 2007; Metcalfe et al., 1994). As carbonate clumped isotopes have a high potential as geohermometer for subsurface applications such as the investigation of diagenesis and the reconstruction of burial depths and fluid flow history, we focus in the following on the effect of low pH on the ^{13}C–^{18}O clumping. Theoretical calculations suggest that Δ_{47} values can be up to 0.03‰ higher at low pH $<$ 4 and 0.01‰ at pH 4–9 compared to the equilibrium composition (Hill et al., 2014). If true, this could impact on the interpretation of Δ_{47} values from subsurface samples that precipitated at lower pH. For example, a deviation of 0.01‰ from the correct calibration corresponds to a relative temperature difference of $\sim$5°C at a mineral formation temperature of 60°C (using the Δ_{47}-T relationship of Kluge et al., 2015).

The precipitation of carbonates at low pH and reasonably high growth rates in the laboratory is difficult (due to low CO_3^{2-} and HCO_3^- concentrations and the slow conversion of $CO_{2,aq} \leftrightarrow H_2CO_3$) and, thus, natural samples that grew under well-monitored conditions can provide attractive material for investigation of this relevant question. In this study, we analyzed carbonates, almost entirely calcite, derived from natural hydrothermal vents and deep geothermal wells in Italy, Hungary, and Turkey. The related hydrothermal waters precipitating calcium carbonate are well characterized and provide a broad range of temperatures (33–100°C) under slightly acidic conditions (pH values 6.1–6.8), as well as typical surface pH conditions (7.4 and 7.5) for comparison, enabling the investigation of a potential speciation effect on ^{13}C–^{18}O clumping relevant to most carbonate forming systems. Stronger effects would only be expected at much lower pH $<$ 4 or significantly higher pH $>$ 11.

2. Sites and Samples

Calcium carbonate samples were collected at natural hydrothermal springs depositing travertine successions at Bagni San Filippo (Italy; Kele et al., 2015) and at the Beltes-2 springs at Pamukkale (Turkey; Kele et al., 2011), from thermal wells in Egerszalók (Hungary; Kele et al., 2008), from a well-head pipe at Karahayit in Pamukkale (Turkey; Kele et al., 2011), and at or near well-head pipes of three man-made deep geothermal wells in Hungary used for thermal water and heat/energy extraction (SCA-CL1, SCA-CL2, SCA-CL3, and SCA-CL4). The latter boreholes of different but steady hydrochemical and operational conditions provide (unwanted) rapidly forming $CaCO_3$ precipitates ("geothermal scaling") constituting an interesting chemical-sedimentary archive for fundamental stable/clumped isotopic studies (Boch et al., 2016; Kele et al., 2015). Two of the geothermal carbonate scales (SCA-CL1 and SCA-CL2) precipitated recently (year 2014) from thermal water of a ca. 1,000 m deep well (53°C at outflow, 45°C after flow through pipe) located in Bük (NW-Hungary). Fresh precipitates (year 2014; SCA-CL3) were further collected from a 2012 m deep thermal well (92°C at well-head) of Fábiánsebestyén near Szeged and from a ca. 1,800 m deep borehole ($\sim$100°C; SCA-CL4) at Kakasszék (both SE-Hungary). In case of deep hydrothermal waters, pressure reduction with

Table 1
Sampling Location, Water Parameters, and Mineralogy of the Collected Precipitates

Location, Sample	Distance from vent (m)	T (°C)	pH	Ca water (mg/L)	Mg water (mg/L)	TDS (mg/L)	Mineralogy	Growth rate (mm/yr)
Egerszalók, E-1	0	67 ± 2	6.12	146.6	24.33	1,535	Calcite 98%	~300
Egerszalók, E-2	0.5	64 ± 2	6.6	148.1	24.55	1,535	Calcite 98%	~300
Bagni San Filippo BSF-1	0	50 ± 2	6.62	n.d.	n.d.	n.d.	Calc. 80%, Arag. 15%, Gypsum 5%	~2
Pamukkale, Bel-2b	155	33.2/33.4[a] ± 2	6.8/6.1[a]	446.4	93.6	1,188	Calcite 100%	n.d.
Karahayit, KH-1	0	51 ± 2	6.2	537	117	n.d.	Calcite 100%	n.d.
SCA-CL1	2	53 ± 3	6.5–6.7	327.1	57.7	7,664	Calcite 99%	~4
SCA-CL2	~500	45 ± 3	6.5–6.7	351.3	58.7	7,776	Calcite 99%	Up to 50
SCA-CL3	2	92 ± 3	7.5	4.6	1.0	3,160	Mg-calcite 99%	n.d.
SCA-CL4	3	100 ± 3	7.4	5.8	0.9	3,985	Mg-calcite 99%	Up to52

Note. For additional information regarding the sample locations and geochemical parameters see Kele et al. (2008, 2011, 2015) and Boch et al. (2016). n.d. = not determined or not precisely known. TDS: total dissolved solid content. The temperature uncertainty is an estimate for the temperature stability over months to a few years.
[a]Parameters at the vent.

concomitant bubble formation related to CO_2 outgassing and boiling (H_2O) is the main process that induces supersaturation and subsequently causes carbonate mineral precipitation.

In order to prevent potential kinetic isotope effects related to fast and extensive CO_2 degassing at the surface or isotopic changes due to Rayleigh-dependent DIC evolution downstream (under equilibrium or kinetic conditions), the samples were taken directly at the natural vents (Bagni San Filippo, see Table 1) or at the well-heads (Egerszalók, Karahayit; SCA-CL1, SCA-CL3, and SCA-CL4) or when impossible, at the location of first carbonate precipitation (Beltes 2 spring, sample Bel-2b, 155 m from vent; SCA-CL2, some hundreds of meters from well-head).

The majority of the samples consist of almost pure calcite (>98%, Table 1). The samples from the deep geothermal wells (SCA-CL1 to SCA-CL4) contain very small amounts (≤1 wt %) of silica (quartz). The samples from NW-Hungary (SCA-CL1 and SCA-CL2) consist of low-Mg-calcite (≤2 mol % $MgCO_3$) while the samples from SE-Hungary (SCA-CL3 and SCA-CL4) consist of Mg-calcite (7–8 mol % $MgCO_3$). Sample BSF-1 consists of 80% calcite, 15% aragonite, and 5% gypsum. The temperatures at the sampling points ranged between 33.2°C (Bel-2b) and 100°C (SCA-CL4) with pH values between ca. 6.1 and 7.5 (Table 1). The waters yielded a relatively broad range of compositions but generally low to moderate Mg concentrations (1–120 mg/L) and low to moderate Ca concentrations (5–540 mg/L). The deep thermal waters precipitating the SCA-CL1 and SCA-CL2 calcite (NW-Hungary) are of the Na-HCO_3-Cl type, while the deep aquifers in SE-Hungary (SCA-CL3 and SCA-CL4) are dominated by Na-HCO_3 thermal waters entailing carbonate scaling. Further details regarding sampling, site description, and hydrochemical characteristics are given in Kele et al. (2008, 2011, 2015). The geothermal scale sample SCA-CL2 was collected from a plastic pipe originally fixed at an auxiliary outlet of a thermal water transport pipeline several hundreds of meters away from the well-head of the deep geothermal well. Similarly, the travertine sample Bel-2b, that represents the first precipitate at the hydrothermal spring of the Beltes section at Pamukkale, formed not directly at the vent but at 155 m distance from the discharge point. Due to the high water flow rate in a covered concrete channel (120 L/s at the Beltes Spring) with near-constant temperature it is therefore likely that the DIC, although attaining chemical equilibrium, did not have sufficient time to isotopically reequilibrate to the new pH conditions and still reflects the initial vent conditions (see supporting information Text S1). We therefore evaluate this sample using the vent parameters.

3. Methods

3.1. Sample Treatment for Carbonate Clumped Isotope Analysis

Five to six milligrams of carbonate (at Imperial College, London) and ~2 mg (at Heidelberg University), respectively, were inserted into the inlet tubing located on the side of a glass reaction vessel containing 1.5–2 mL of 105% phosphoric acid in the main chamber. The reaction vessel was evacuated for 30 min and typically reached pressures of 10^{-1} to 10^{-2} mbar before the acid digestion was started by dropping the

sample from the inlet part into the main chamber that contains the acid. At 90°C, calcite was digested by phosphoric acid for 10 min in the stirred reaction vessel, and the evolving CO_2 was immediately and continuously collected in a N_2-cooled glass trap. Each sample was placed in an individual reaction vessel that was replaced and cleaned after the phosphoric acid reaction was completed.

The reactant CO_2 was purified using a procedure analogous to that of Dennis and Schrag (2010). In brief, after trapping the evolved gases, a first cryogenic distillation step was followed by separation of CO_2 and water using a dry-ice ethanol cooled glass trap. The remaining gas was then passively passed through a trap densely packed with Porapak Q (porous polymer adsorbent) held at −35°C. The purified CO_2 gas was afterward captured in a freezing finger and immediately transferred to the mass spectrometer for analysis.

3.2. Mass Spectrometric Analysis and Data Evaluation

The mass spectrometric sample analysis was done using two different isotope ratio mass spectrometers: a MAT 253 (Thermo Scientific) in the Qatar Stable Isotope Laboratory at Imperial College and a MAT 253 Plus at Heidelberg University. The analysis followed the procedures described by Huntington et al. (2009) and Dennis et al. (2011). A measurement consisted of eight acquisitions with 10 cycles per acquisition (26 s integration time per individual cycle). Each acquisition included a peak center, background measurements, and an automatic bellows pressure adjustment aimed at a 15 V signal at mass 44 at Imperial College and 6 V at Heidelberg University. The sample gas was measured against an Oztech reference standard at Imperial College and an internal working gas standard at Heidelberg University. Heated gases (~1,000°C), water-equilibrated gases (25°C, 50°C, 80°C) and a Carrara marble carbonate standard were analyzed regularly to transfer the measured values into the absolute reference frame (Dennis et al., 2011). ETH carbonate standards (Kele et al., 2015; Meckler et al., 2014; Müller et al., 2017) were measured frequently to additionally monitor the accuracy of the reference frame transfer. Sample contamination was monitored using the mass 48 and mass 49 signal based on methods described in Affek and Eiler (2006) and Huntington et al. (2009). Δ_{48} deviations above 2‰ from the Δ_{48}-δ^{48} regression of clean standards and samples and values of the 49 parameter ($(R^{49}_{sample} - R^{49}_{WG}) * 10^4$) above 0.5 were generally deemed contaminated and not used for interpretation (see also Davies & John, 2017). In few cases elevated Δ_{48} values were observed together with a normal 49 parameter. Additional cleaning (e.g., passing the gas twice through the preparation line and the Porapak trap) reduced the Δ_{48} value, but did not impact on the Δ_{47} value. Together with a normal 49 parameter, it suggests that sulfate fragments were released that did not influence the clumped isotope value and those Δ_{47} values were therefore considered during the data evaluation. Δ_{47} values are linearity-corrected using heated gas data (Huntington et al., 2009) before transferring them into the absolute reference frame of Dennis et al. (2011). The free software "Easotope" (John & Bowen, 2016) was used for clumped isotope calculations and corrections at Imperial College and an Excel-based system at Heidelberg University, applying the isotope parameters after Gonfiantini et al. (1995). Assessing the updated isotope parameters of Brand et al. (2010) for evaluation did not show large differences for the selected data set (supporting information). In addition, the Δ_{47}-T relationship of Kluge et al. (2015) has been established based on the Gonfiantini et al. (1995) parameter. For better comparability, we therefore use the Gonfiantini parameters here. Due to a zero-slope Δ_{47}-δ_{47} relationship at Heidelberg no linearity-correction was performed there. For acid digestion at 90°C we used a correction of 0.069‰ for calcite (based on Guo et al., 2009) after the data transfer to the absolute reference frame. A similar value of about 0.07‰ was also found in the experimental study of Wacker et al. (2013). The acid digestion correction varies in different experimental studies from 0.07 to 0.09‰ (e.g., Defliese et al., 2015; Passey & Henkes, 2012; Tang et al., 2014; Wacker et al., 2013). To maintain comparability with the Δ_{47}-T calibration of Kluge et al. (2015), we kept the same acid digestion correction of 0.069‰. All Δ_{47} values are reported in the absolute reference frame of Dennis et al. (2011) and are compared to the carbonate clumped isotope calibration of Kluge et al. (2015):

$$\Delta_{47} = 0.98 \times \left(-3.047 \times 109/T^4 + 2.365 \times 107/T^3 - 2.60 \times 10^3/T^2 - 5.88/T\right) + 0.293 \quad (1)$$

We use the experimental Δ_{47}-T relationship of Kluge et al. (2015) as calibration reference as it was prepared and measured with the same analytical techniques as the hydrothermal samples of this study at Imperial College and as it follows closely the theoretical predictions of Guo et al. (2009). Recent studies show that at least all inorganic precipitates, including the carbonates from Kluge et al. (2015) up to 100°C, adhere to one universal calibration line if the same acid reaction temperature and procedure is used (Bonifacie et al., 2017; Kelson et al., 2017). For example, using the Kele et al. (2015) Δ_{47}-T relationship results in only minor changes

Table 2
Clumped, Carbon and Oxygen Isotope Results of the Hydrothermal Calcite Samples

Location, Sample	Δ_{47} (‰)	Δ_{47} offset (‰)	$\delta^{18}O_{VPDB}$ (‰)	$\delta^{18}O_{VSMOW}$ (‰)	$\delta^{18}O$ offset (‰) Kim and O'Neil	$\delta^{18}O$ offset (‰) Tremaine	$\delta^{13}C_{VPDB}$ (‰)	$\delta^{18}O_{water}$ (‰)	*n*
pH < 7									
Egerszalók, E1	0.607 ± 0.006	0.013 ± 0.006	−19.14 ± 0.03	11.19	1.50	−0.64	2.63 ± 0.03	−10.9	3
Egerszalók, E2	0.629 ± 0.013	0.030 ± 0.013	−19.27 ± 0.15	11.05	0.86	−1.24	2.40 ± 0.05	−10.8	4
Bagni San Filippo, BSF 1	0.626 ± 0.007	−0.006 ± 0.007	−13.26 ± 0.06	17.25	1.81	−0.03	4.63 ± 0.03	−8.0	5
Pamukkale, Bel 2-b	0.677 ± 0.009	0.003 ± 0.009	−11.73 ± 0.13	18.82	0.89	−0.63	5.23 ± 0.06	−8.5	3
Karahayit, KH-1	0.625 ± 0.003	−0.003 ± 0.003	−13.14 ± 0.15	17.37	2.02	0.15	5.76 ± 0.05	−7.8	3
SCA-CL1	0.647 ± 0.008	0.023 ± 0.008	−16.89 ± 0.09	13.50	1.70	−0.20	2.03 ± 0.05	−11.1	3
SCA-CL2	0.637 ± 0.008	−0.006 ± 0.008	−16.56 ± 0.45	13.85	0.66	−1.09	2.67 ± 0.17	−10.4	3
Mean samples pH <7		0.008 ± 0.015			1.5 ± 0.5	−0.4 ± 0.5			
pH > 7									
SCA-CL3	0.546 ± 0.007	−0.003 ± 0.007	−24.48 ± 0.36	5.68	0.6	−1.95	−1.59 ± 0.05	−12.0	3
SCA-CL4	0.538 ± 0.022	0.005 ± 0.022	−22.39 ± 0.56	7.83	2.3	−0.39	−0.86 ± 0.30	−10.3	3
Mean samples pH>7		0.001 ± 0.005			1.4 ± 1.2	−1.2 ± 1.0			

Note. The Δ_{47} offset is calculated with regard to equation (1), the $\delta^{18}O$ offset relative to the water $\delta^{18}O$ value (Kele et al., 2008, 2011), measured water temperature and the fractionation factors of Kim and O'Neil (1997) and Tremaine et al. (2011), respectively. *n* gives the number of replicates measured per sample. The uncertainty is given as standard error for Δ_{47}, $\delta^{18}O$, and $\delta^{13}C$ values based on the replication of sample aliquots.

in the inferred temperatures and offsets ($\leq$ 0.008‰ for T = 30–70°C). For best comparability and to avoid small process-dependent and calibration-dependent biases we choose to use the Δ_{47}-T relationship of Kluge et al. (2015) that extends over the longest temperature range of all laboratory calibration studies based on inorganic calcite precipitates.

Samples that were analyzed in both laboratories (SCA-CL1–SCA-CL4) are generally consistent in Δ_{47} and $\delta^{13}C$ (visible in the small standard deviation of the mean). $\delta^{18}O$ values are comparable but show a higher scatter. The external reproducibility of standards is similar for both laboratories at 20 ppm for Δ_{47} (1σ standard deviation), 0.2‰ for $\delta^{18}O$ and 0.1‰ for $\delta^{13}C$, respectively (1σ; see also Kluge et al., 2015; Kluge & John, 2015).

4. Results

The stable oxygen and carbon isotope ratios of our hydrothermal calcites from vent locations exhibit a wide range of values between −24.5‰ and −11.7‰ (VPDB) for $\delta^{18}O$ and −1.6‰ to 5.8‰ for $\delta^{13}C$ (VPDB; Table 2). Carbonate $\delta^{18}O$ values scatter around expected values (deviations between −1.95 and +0.15‰) following the empirical $CaCO_3$-H_2O fractionation factor of Tremaine et al. (2011), the respective hydrothermal water $\delta^{18}O$ values, and the measured in situ water temperatures (Table 2; Kele et al., 2008, 2011). Using instead the experimental $CaCO_3$-H_2O fractionation factor of Kim and O'Neil (1997) carbonate $\delta^{18}O$ values would show a small positive offset from expected values of +0.6‰ to 2.3‰. Recent studies show that the fractionation factor of Kim and O'Neil (1997) may not perfectly represent natural conditions and we therefore compare measured and calculated $\delta^{18}O$ based on newer studies focusing on travertines and speleothems (Demény et al., 2010; Kele et al., 2015; Tremaine et al., 2011). The reader is reminded of the ongoing discussion on the oxygen isotope $CaCO_3$-H_2O fractionation (e.g., Coplen, 2007; Dietzel et al., 2009; Kluge et al., 2014; Watkins et al., 2014). Δ_{47} values vary between 0.538 ± 0.022‰ and 0.677 ± 0.007‰ and mostly show negligible offsets from equilibrium based on equation (1), independent of pH (Figure 1). Only three out of nine samples yield slightly elevated offsets (+0.014 ± 0.006‰, +0.030 ± 0.013‰, +0.023 ± 0.008‰, ±1SE). The highest Δ_{47} offset is related to the highest growth rate of the investigated samples. Similarly, $\delta^{18}O$ offsets from the reference line of Tremaine et al. (2011) follow a growth-rate dependence with highest offsets being correlated to the fastest growth (Tables 1 and 2). $\delta^{13}C$ values exhibit no significant correlation with pH and with $\delta^{18}O$ offsets (supporting information Figure S1).

5. Discussion

Mineral growth rates are essential for discussing potential pH-related effects in Δ_{47} and $\delta^{18}O$ values. We define growth rates in three main categories: as *high* if growth exceeds rates of 10^{-5} mol/(m^2 s) (in the

following also termed rapid or fast growth), as *intermediate* between 10^{-7} and 10^{-5} mol/(m^2 s), and as *slow* below 10^{-7} mol/(m^2 s). For example, laboratory-based mineral formation mostly corresponds to the intermediate growth regime (Watkins et al., 2014). In contrast, the natural Devils Hole vein calcite corresponds to slow growth with $\sim 6 \times 10^{-10}$ mol/(m^2 s) (Kluge et al., 2014), approaching equilibrium conditions (Watkins & Hunt, 2015).

High carbonate precipitation rates relative to DIC equilibration times are a prerequisite for preserving disequilibrium Δ_{47} values as rapid precipitation prevents isotopic equilibration between the DIC and water and among the DIC species (e.g., Hill et al., 2014; Saenger et al., 2012). This effect is of particular importance for biologically mediated carbonate formation. Low temperatures and higher pH values correspond to long isotope equilibration times (see section 5.4). Significant pH changes in the calcifying fluid lead to changes in the DIC speciation and are combined with intermediate to high carbonate precipitation rates (e.g., Al-Horani et al., 2003; Cohen & McConnaughey, 2003; de Nooijer et al., 2009; McConnaughey, 2003; Saenger et al., 2012; Venn et al., 2011). Carbonate precipitation rates can also be high for inorganic carbonates such as at hydrothermal springs or in their downstream sections and reaches vertical extension rates of up to 1 mm per day (e.g., Fouke et al., 2000; Kele et al., 2008). In case of the studied hydrothermal vents precipitation rates determined for the hydrothermal calcites at Bagni San Filippo ($\sim$1.5 mg cm^{-2} d^{-1}, about 2×10^{-6} mol (m^2 s)$^{-1}$) and at Kakasszék (SCA-CL4; $\sim 4 \times 10^{-5}$ mol (m^2 s)$^{-1}$) are in the upper range compared to typical laboratory experiments (compare Watkins and Hunt, 2015) or far beyond. Vertical mineral growth of 1–10 mm/yr (10^{-1} to 10 μmol (m^2 s)$^{-1}$) is typically observed for carbonate scales in pipes of deep geothermal wells (e.g., Boch et al., 2016) which should provide the potential to record isotopic disequilibrium of the DIC in the precipitating mineral.

5.1. Assessment of the pH Influence on ^{13}C–^{18}O Clumping

Vent carbonates in the investigated pH range (pH 6–8) are scattering around the expected clumped isotope values at the respective water discharge temperature (mean offset 0.006 ± 0.004‰; 1SE, $n = 9$). A few samples yield slightly higher positive offsets partially related to high growth rates (Table 2). The offset direction and magnitude is unrelated to the calibration choice. Most vent calcite Δ_{47} values have been determined in the same laboratory with the same analytical procedures as was used for the Kluge et al. (2015) calibration line enabling an optimal comparability. Furthermore, the calibration line of Kluge et al. (2015) is consistent with the range of other synthetic calcites that were precipitated at <100°C (Kelson et al., 2017) and yielded good correspondence with fluid inclusion thermometry (MacDonald et al., 2015), Uk'37 temperatures (Drury & John, 2016) and other independent geological thermometers (Garcia del Real et al., 2016). Evaluating the data of this study with the Kele et al. (2015) relationship only causes insignificant variations (0.007 ± 0.004‰). Similarly, evaluating the Kele et al. (2015) data using the Δ_{47}-T calibration of Kluge et al. (2015) only causes minor changes (supporting information Figure S2).

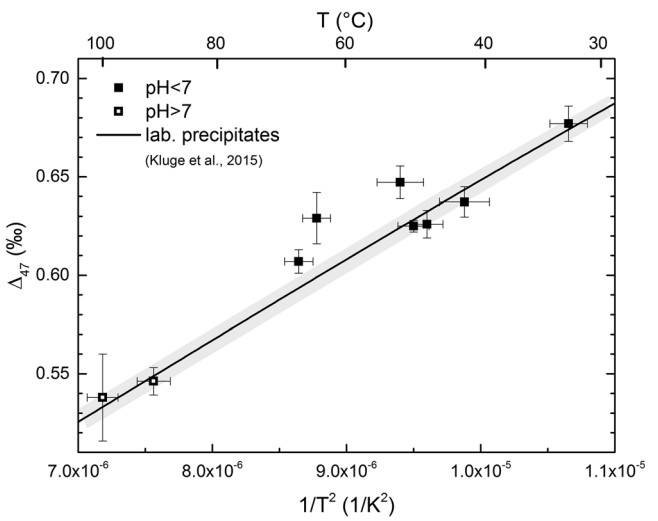

Figure 1. Vent calcite Δ_{47} values of samples precipitated at pH < 7 (filled squares) and pH >7 (open squares) relative to the Δ_{47}-T calibration (continuous line) determined by inorganic precipitates in the same laboratory (Kluge et al., 2015). The gray shaded area represents the uncertainty of the Δ_{47}-T calibration. The Δ_{47} error bars represent the standard error of each sample.

Evaluating the vent calcite data set as a whole irrespective of individual growth rates a small disequilibrium effect on the order of 0.01‰ appears possible. The average Δ_{47} offset of +0.006 ± 0.004‰ (1 SE, $n = 9$) of all vent calcites is consistent with theoretical calculations of Hill et al. (2014) that predict a maximum difference of +0.01‰ between the equilibrium calcite value and the equilibrium DIC Δ_{47} value obtained during rapid precipitation at low and intermediate pH values of ca. 4–10. The absence of larger offsets may be due to the missing or only small additional influence of carbonic acid (H_2CO_3), which can be transformed to CO_3^{2-} ions that are incorporated during mineral formation and that were predicted to yield deviations of up to +0.04‰.

At pH 6.0–6.6, the DIC is changing from a HCO_3^--dominated system to a system dominated by dissolved CO_2 and H_2CO_3 (Figure 2). Although high Na^+ and Cl^- concentrations were found not to directly impact on Δ_{47} (Kluge & John, 2015), salinity can slightly influence the DIC speciation and for increasing salinity the DIC pattern is shifted to lower

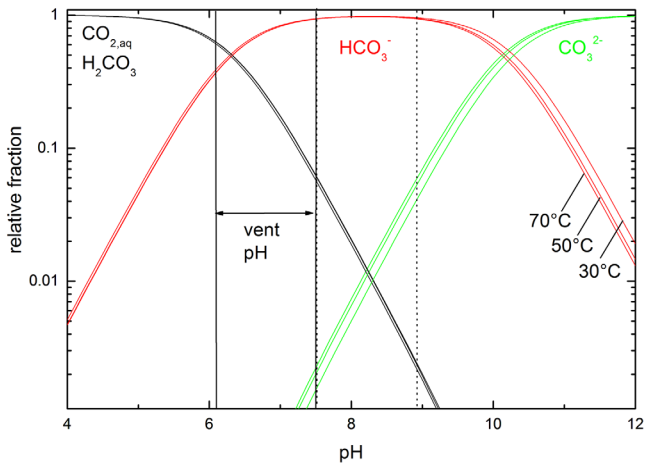

Figure 2. Distribution of the DIC species ($CO_{2,aq}$, H_2CO_3, HCO_3^-, CO_3^{2-}) at different pH values and temperatures relevant to the studied hydrothermal carbonate samples. Calculations are based on Millero et al. (2006). The calculation at 70°C is an extrapolation of the data set of Millero et al. (2006) and is given for illustration of the temperature effect on the speciation in the range of the studied hydrothermal vents. The vertical dotted lines indicate the typical pH range of laboratory carbonate precipitates. Between pH 5 and pH 9 a maximum offset of +0.01‰ is expected for fast precipitating minerals.

pH values (up to 90–110 g/L in a NaCl-dominated solution, for higher salt concentration the pattern shifts back to the initial conditions, see e.g., Millero et al., 2007). For example, at zero salinity the maximum HCO_3^- fraction is at pH 8.3 whereas it shifts to 8.0 at seawater salinity and to 7.7 at a NaCl concentration of ~100 g/L (all at 30°C). The total dissolved solid content for all investigated hydrothermal systems is below 8 g/L causing no significant shift in the DIC speciation relative to zero salinity (supporting information Figure S3). We therefore use the zero salinity DIC speciation as reference. The ^{13}C–^{18}O bond abundance of the different DIC species varies given their different structure and vibrational frequencies (e.g., Hill et al., 2014). Rapid carbonate precipitation from a system with very low initial pH < 4 that is dominated by H_2CO_3 is expected to lead to a positive offset on the order of 0.04‰ (Hill et al., 2014). At the hydrothermal vents with pH values of 6.1–6.8, between 32% and 62% of the DIC comprises of dissolved CO_2 and H_2CO_3. Neglecting contributions from H_2CO_3 as suggested by Hill et al. (2014) the total estimated Δ_{47} deviation is constant at +0.010‰ within the whole investigated pH range as the potential offset is 0.01‰ for the calcite fraction that precipitates rapidly from a HCO_3^- dominated solution compared to slow isotopically equilibrated mineral formation (Hill et al., 2014). Temperature has a minor influence on the difference between the DIC species in the range from 30 to 100°C (changes are ~2 ppm for clumped isotopes, Hill et al., 2014). We therefore neglect it in the following discussion. In general, the clumped isotope difference between the DIC species decreases with increasing temperatures and is already reduced to the low ppm range at 500°C (Hill et al., 2014). Similarly, the difference of the $\delta^{18}O$ value between the DIC species also changes with temperature and generally decreases with increasing temperature (supporting information Figure S4). The empirical average Δ_{47} offset of the studied hydrothermal vent precipitates is +0.006 ± 0.004‰ and, thus, broadly consistent with the theoretical prediction in the investigated temperature range.

As also pointed out by Hill et al. (2014) and Watkins et al. (2014), the individual growth rate is decisive if the DIC clumped isotope value is directly inherited. The growth rate of the investigated samples span the range from 10^{-7} to 10^{-4} mol/(m^2 s), including all samples with known growth rate from the study of Kele and Hunt (2015) from 10^{-7} to 10^{-4} mol/(m^2 s). The data of Kele et al. (2015) was evaluated for consistency relative to equation (1). A comparison with the theoretical prediction of Watkins and Hunt (2015) shows scattering of individual data points around expected values (Figure 3). Starting at 10^{-8} mol/(m^2 s) at pH 8 or 10^{-7} mol/(m^2 s) at pH 7 increasing offsets of up to 0.01‰ at the highest growth rates above 10^{-4} mol/(m^2 s) are expected. Calculating average values for defined growth intervals (<10^{-6}, 10^{-6} to 10^{-5}, 10^{-5} to 10^{-4} mol/(m^2 s), respectively) provides a more coherent picture. In all three intervals, the average is well corresponding to the theoretical prediction at pH 7 or pH 8 with values of 0.003 ± 0.003‰ (1SE, $n = 4$) for <10^{-6} mol/(m^2 s), 0.005 ± 0.006‰ (1SE, $n = 4$) for 10^{-6} to 10^{-5} mol/(m^2 s), and 0.014 ± 0.007‰ (1SE, $n = 5$) for 10^{-5} to 10^{-4} mol/(m^2 s), respectively. The uncertainty is still elevated and limits the interpretation, however, it suggests that the highest growth rates above 10^{-5} mol/(m^2 s) likely involve a Δ_{47} offset in the predicted 0.01‰ range. This is corroborated by a similar effect in the $\delta^{18}O$ values of the same samples (see section 5.2).

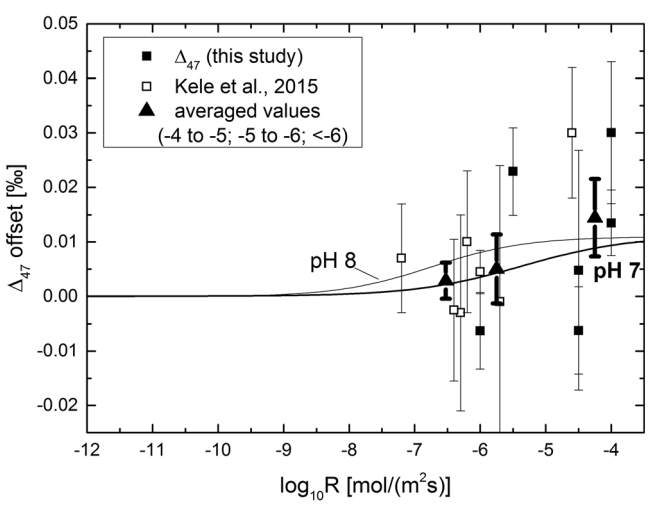

Figure 3. Δ_{47} offsets (measured minus expected value) versus growth rate. The continuous lines illustrate the theoretically expected Δ_{47} offsets at pH 7 and pH 8 for rapidly growing carbonates (using theoretical offset estimates of Watkins & Hunt, 2015) relative to slowly precipitated calcite that would follow the laboratory reference. The Δ_{47} offset was calculated relative to the water temperature and equation (1). Open squares refer to data points from the study of Kele et al. (2015).

5.2. Effect of pH on $\delta^{18}O$ in Fast Precipitating Carbonates

Vent carbonate $\delta^{18}O$ values are consistent with expected equilibrium values or slightly more negative following the fractionation curve of

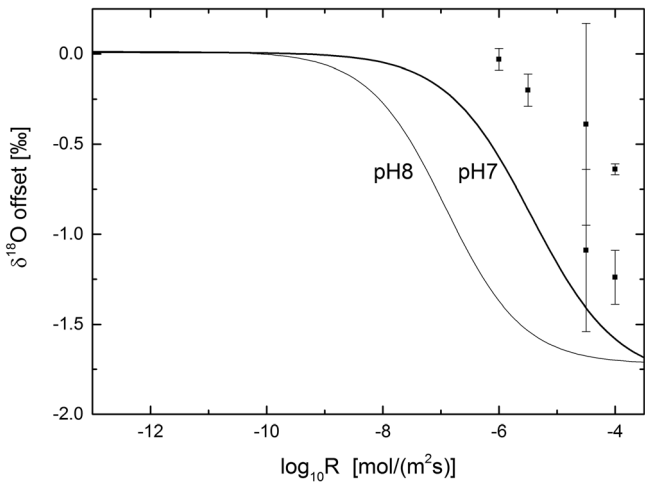

Figure 4. $\delta^{18}O$ offsets of hydrothermal calcite samples (relative to the fractionation factor of Tremaine et al. (2011) versus growth rate. The continuous lines are theoretical predictions based on the growth rate-dependent evolution of $\delta^{18}O$ following Watkins and Hunt (2015).

Tremaine et al. (2011) (see also Kele et al., 2015) and with a small positive offset relative to the Kim and O'Neil (1997) experimental data. Following recent literature, we chose the reference data of Tremaine et al. (2011) for further discussion. Note that the DIC-speciation effect and its growth-rate dependence should be independent of the chosen fractionation factor $\alpha_{CaCO_3-H_2O}$.

A change in the DIC speciation at lower pH should lead to more positive $\delta^{18}O$ values if carbonate is rapidly formed. Zeebe (1999) determined $\delta^{18}O$ values to be higher by $\sim$2.5‰ at pH 6 compared to pH 8 (for a constant aqueous solution temperature of 19°C). As for Δ_{47}, the mineral growth rate is critical for its expression in the measured calcite $\delta^{18}O$ value. Starting at 10^{-8} mol/(m^2 s) at pH 8 or 10^{-7} mol/(m^2 s) at pH 7 negative offsets relative to slowly growing carbonates of up to -1.7‰ at the highest growth rates above 10^{-4} mol/(m^2 s) are expected (Watkins & Hunt, 2015). Our $\delta^{18}O$ offsets tend in the expected negative direction and are of the same magnitude (-0.03‰ to -1.95‰, Figure 4). A comparison with the theoretically predicted $\delta^{18}O$ offsets shows a correlation with growth rate. The offsets are more negative at faster growth, but do not generally fit to the predicted curves at pH 7 or pH 8 and likely correspond to the evolution at pH 6 or lower (Figure 4). At high growth rates, as given for most of the hydrothermal calcite precipitates in this study (Table 1), ^{16}O is preferentially incorporated into the mineral causing lower $\delta^{18}O$ values (DePaolo, 2011; Dietzel et al., 2009; Gabitov, 2013; Gabitov et al., 2012; Watkins et al., 2014; Watson, 2004).

In contrast to $\delta^{18}O$, $\delta^{13}C$ values cannot be easily correlated to pH or growth rate as the individual hydrothermal vent samples originate from different regions with distinct bedrock geologies and aquifers, different CO_2 sources and hydrothermal activities (supporting information Figure S1).

5.3. Other Potential Influences on Hydrothermal Vent Carbonate $\delta^{18}O$ and Δ_{47} Values

The isotopic values of hydrothermal vent calcites could generally be influenced by additional mechanisms beyond pH-related DIC speciation, such as fast CO_2 degassing (Daëron et al., 2011; Kele et al., 2011), fast temperature changes of the discharging water close to the vent or by mixing of thermal water with cooler meteoric fluids.

Fast degassing of CO_2 from hydrothermal water could cause positive offsets (Kele et al., 2011). In contrast, all vent carbonate $\delta^{18}O$ values are more negative compared to expected values based on fractionation factors of Tremaine et al. (2011; -0.03‰ to -1.95‰; Table 2), rejecting a significant influence of CO_2 degassing. A potential disequilibrium due to fast CO_2 degassing would also affect Δ_{47} values and lead to negative deviations from clumped isotopic equilibrium (Affek et al., 2008, 2014; Daëron et al., 2011; Kluge & Affek, 2012; Kluge et al., 2013; Meckler et al., 2009; Wainer et al., 2011). For speleothems, Δ_{47} and $\delta^{18}O$ values appear to be correlated with a decrease of $\sim$0.05‰ in Δ_{47} per 1‰ increase in the carbonate $\delta^{18}O$ value (Kluge et al., 2013). In contrast, the investigated hydrothermal vent calcite Δ_{47} and $\delta^{18}O$ offsets show no statistically relevant correlation with each other (supporting information Figure S5). Thus, the underlying mechanism for the isotope offsets observed in the hydrothermal vent precipitates presented here is clearly different from speleothems and suggests that rapid CO_2 degassing is not the primary cause. It does not exclude limited chemical and isotopic changes due to CO_2 degassing at the studied hydrothermal vents, however, the magnitude of effects of degassing are likely small owing to the much thicker water layers (travertine deposits) or pressurized water flow in transport pipes (geothermal scale samples; e.g., Boch et al., 2016) and the typically large amounts of thermal water discharged (Pamukkale springs: $\sim$4,500 L/min; Egerszalók: 875 L/min; Bagni San Filippo: 6–1,200 L/min, Frondini et al., 2008; Minissale, 2004); SCA-CL1: $\sim$720 L/min; SCA-CL3: 750–1,250 L/min; SCA-CL4: $\sim$500 L/min).

It is important to note that *downstream* travertine samples at the locations of this study show an isotopic pattern similar to speleothems (Figure 5). pH values of the related water in the downstream section are in the typical range above pH 7; i.e., progressively increased compared to initial values at the vent. In particular, $\delta^{13}C$ values increase strongly downstream and reach shifts of up to $+6$‰ relative to initial values (Figure

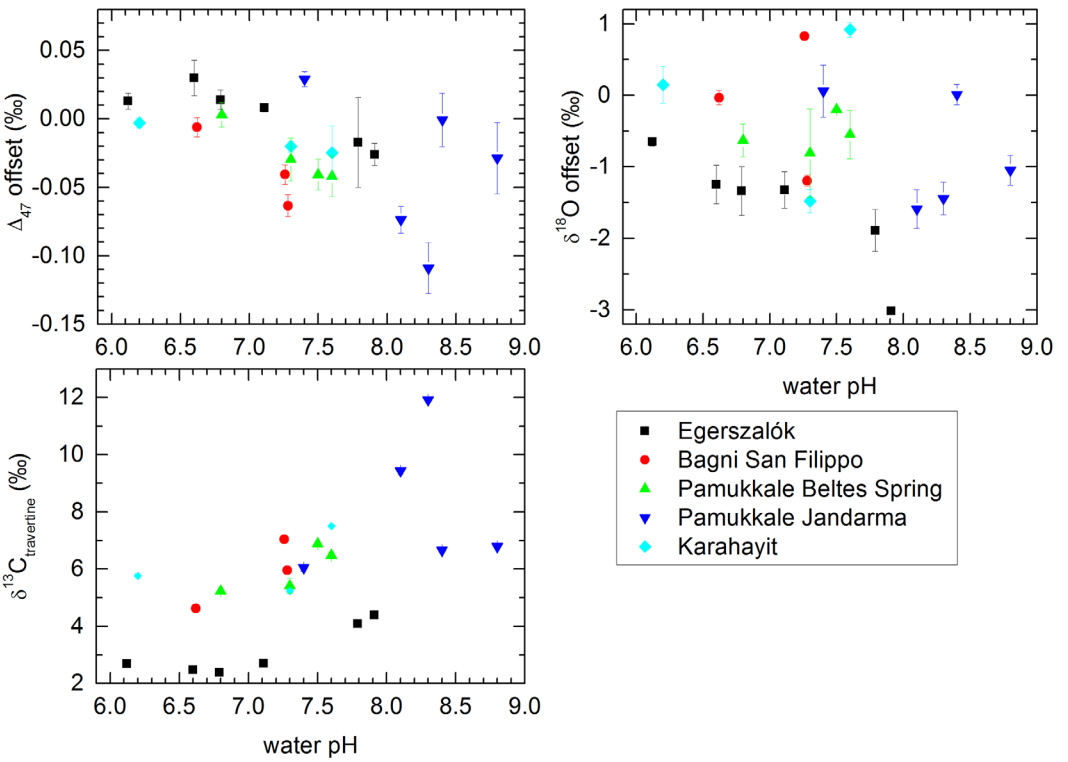

Figure 5. Isotope evolution of natural travertines deposited at the surface in the downstream section of hydrothermal springs of this study (data in the supporting information). Distance from the vent is characterized by chemical changes of the water that can be traced by increasing pH. The highest observed pH at each spring indicates the maximum distance from the thermal water vent. The $\delta^{18}O$ offset is given relative to Tremaine et al. (2011). Using the fractionation factor of Kim and O'Neil (1997) would lead to a general shift of $+1.5$ to $2‰$.

5). Trends in the evolution of the carbonate $\delta^{18}O$ values downstream are less easy to interpret. In contrast to the increasing $\delta^{13}C$ values due to ongoing Rayleigh fractionation of the DIC and CO_2 degassing, travertine $\delta^{18}O$ offsets from expected local isotope equilibrium are getting slightly more negative downstream. This could be due to the rapid mineral precipitation at the downstream slopes and related preferential uptake of ^{16}O in the calcium carbonate mineral, causing increased negative offsets. The observed range of up to $-3‰$ at pH 8 is consistent with predictions by Watkins and Hunt (2015). Δ_{47} values are decreasing strongly downstream and show enhanced negative offsets of up to $-0.11‰$ relative to expected equilibrium values. Comparing $\delta^{13}C$ with Δ_{47} changes shows that a $1‰$ increase of travertine $\delta^{13}C$ in the downstream samples is correlated to a $\sim 0.02‰$ decrease in Δ_{47} (supporting information Figure S6). As the $\delta^{18}O$ value is beyond fast CO_2 degassing and Rayleigh evolution of the solution likely influenced by the mineral-DIC fractionation through rapid growth we do not compare it directly to Δ_{47}. Instead we transfer the $\delta^{13}C$-Δ_{47} relation to the oxygen isotope system by using the kinetic $\delta^{13}C$-$\delta^{18}O$ correlation of unbuffered solutions (slope: 0.52, Mickler et al., 2006). This leads to a $-0.038 \pm 0.008‰$ change in Δ_{47} per $1‰$ increase in $\delta^{18}O$; a value that is consistent with findings from cave samples (e.g., Kluge et al., 2013: Δ_{47}-$\delta^{18}O$ slope of -0.047 ± 0.005) and indicates that the same underlying processes are relevant for carbonate from downstream travertines and stalagmites (see e.g., also Yan et al., 2017), together with a growth-rate dependent kinetic fractionation between DIC and mineral for $\delta^{18}O$.

Another possibility for isotopic changes at the vent location is related to clumped isotope reequilibration following temperature changes of the water. When warm/hot hydrothermal water migrates toward the surface it starts cooling down. Depending on how rapid the cooling proceeds Δ_{47} values will be more or less influenced (for calcite see Henkes et al., 2014). Fast cooling combined with rapid carbonate precipitation does not leave enough time for reordering of ^{13}C and ^{18}O in the C–O bonds in the DIC in correspondence to the new temperature environment and should therefore archive the original high-temperature (i.e., lower Δ_{47}) signal in the forming carbonate minerals. For example, at 60°C the rate constant for CO_2–H_2O exchange is

about 1 h^{-1} (extrapolated from Clog et al., 2015 and Affek, 2013) indicating that equilibrium for dissolved CO_2 still needs hours to be reached. In contrast, all measured Δ_{47} values are similar or higher than expected at the water temperatures of the vent sampling sites and therefore exclude this mechanism as an explanation for the observed clumped isotope offsets.

Mixing of different clumped isotope end-member fractions in heterogeneous carbonates can lead to overestimation or underestimation of the true Δ_{47} value (Defliese & Lohmann, 2015; Eiler & Schauble, 2004). Transferring their findings to clumped isotopes in DIC, mixing of deep hydrothermal water with cooler meteoric fluids could result in more positive Δ_{47} values in DIC due to nonlinear mixing effects of clumped isotopes. Some mixing of deeper thermal water with shallower meteoric water cannot be excluded for the hydrothermal springs in the Pamukkale region as spring temperatures vary by more than 20°C within 1 km (Özkul et al., 2013). In contrast, mixing with cooler fluid in the subsurface is unlikely at Egerszalók as the water is discharged through a well drilled for oil exploration from a depth of ~400 m (Kele et al., 2008). Hydrothermal springs in the vicinity of Bagni San Filippo (Bagni San Filippo-Fosso Bianco, Il Doccio, Bagni di Petriolo) exhibit similar discharge temperatures of 44–50°C and water $\delta^{18}O$ values of $-6‰$ to $-8‰$ (Kele et al., 2015). These similarities over regional distances of 30–50 km argue against significant local water mixing close to the hydrothermal water discharge point. A significant cool meteoric contribution can also be neglected for the thermal waters from geothermal wells tapping deep Pannonian basin (Hungary) aquifers supporting long water residence times and leading to the rapid deposition of the analyzed calcite scales from well-head pipes (SCA-CL1 to CL4; Boch et al., 2016; Szanyi & Kovács, 2010).

5.4. Implications

Carbonates precipitate in the (sub)surface environment and during diagenetic processes at vastly different pH values (5–13; Clark et al., 1992; Gilfillan et al., 2009; Hesse, 1987; Kharaka & Hanor, 2007; Metcalfe et al., 1994). Fast CO_2 degassing of (carbonic) acidic solutions at the surface or CO_2 uptake in alkaline aqueous solutions can cause rapid carbonate formation that has the potential to record isotopic disequilibrium conditions (Falk et al., 2016), for example, related to DIC speciation. A pH-related effect was experimentally observed at higher pH (8–12) (Tripati et al., 2015). Biogenic carbonate precipitation in this range is typically related to an increase in pH toward alkaline values such as in corals and foraminifera (Al-Horani et al., 2003; Cohen & McConnaughey, 2003; de Nooijer et al., 2009; Venn et al., 2011). Increases are mostly limited to 0.5–1 pH units leading to pH values between 8 and 9 (McConnaughey, 2003). Even higher pH values above 10 could lead to a certain pH effect as the dominant DIC species changes from HCO_3^- to CO_3^{2-} (Figure 2). Thus, fast carbonate precipitation from alkaline solutions most likely records a kinetic effect of DIC speciation in the carbonate (Falk et al., 2016). Similarly, our empirical study on low pH hydrothermal vent calcites indicates a small pH-related effect on the carbonate Δ_{47} value at pH 6–8 on the order of $0.01‰$. Highly important are the growth rates as only above a certain threshold offsets become apparent in both $\delta^{18}O$ and Δ_{47} (see Watkins & Hunt [2015] for details). Therefore, applications to natural inorganic samples at pH 6–8 may not be influenced by DIC speciation if the growth is in the slow or intermediate range ($<10^{-6}$ to 10^{-7} mol/(m^2 s)). For natural samples with growth rates above 10^{-5} mol/(m^2 s) a small positive offset in Δ_{47} of up to $0.01‰$ and for $\delta^{18}O$ of up to $-2‰$ may occur and needs to be considered during interpretation.

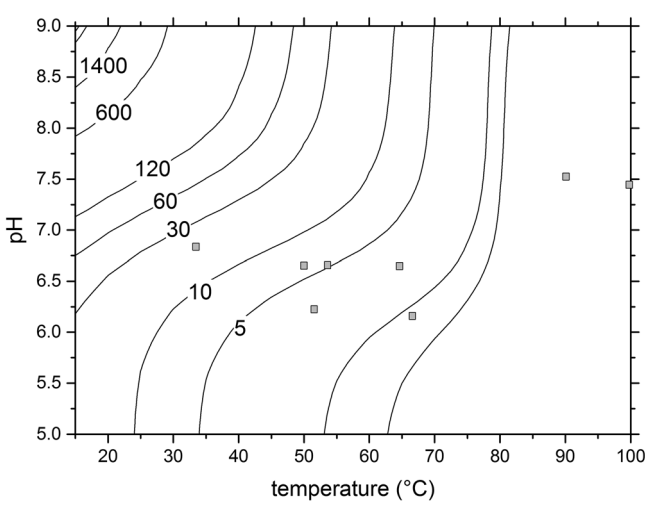

Figure 6. Time intervals for oxygen isotope equilibration between DIC and water (contour lines in minutes to reach 99% equilibrium) in relation to pH and solution temperature. The calculations are based on Uchikawa and Zeebe (2012) for negligible salinity. The carbonate growth conditions of this study are marked by gray squares. Note that the equilibration times given above 60°C are extrapolations beyond the range of the experimentally assessed rate constants.

An interesting aspect is the threshold growth rate beyond that isotope effects get recorded in the forming mineral. The threshold is generally increasing with decreasing pH (see Figures 3 and 4 or Watkins & Hunt, 2015). An explanation could be related to the time scales necessary for isotopic equilibration in the DIC and between DIC and the solution. The time required for equilibration is dependent on temperature and pH, with generally faster equilibration times at lower pH and higher temperatures (Figure 6; e.g., Watkins et al., 2013). The time required to reach 99% equilibrium is reduced by more than one order of magnitude at $pH \leq 6$ compared to pH 8 (Figure 6).

Furthermore, isotopic equilibration proceeds within less than 1 min at 100°C (extrapolating the data of Beck et al., 2005). In addition, the differences in Δ_{47} and $\delta^{18}O$ between the DIC species decrease rapidly for temperatures above 100°C (Hill et al., 2014). Thus, the potential to record disequilibrium in diagenetic carbonates due to pH speciation effects decreases with decreasing pH and increasing temperature, for example, with increasing burial depth in a sedimentary basin. On the other hand, the time required for equilibration of the oxygen isotopes (DIC species and water) increases rapidly with pH (see e.g., Uchikawa & Zeebe, 2012) and therefore suggests carbonate formation at higher pH and lower temperatures to be most susceptible to pH-related effects.

A high mineral growth rate and slow isotope equilibration are prerequisite for the pH effect to be preserved in the precipitated mineral and are the most likely explanation why the pH effect was detected in biogenic carbonates and carbonates from alkaline solutions, but was not observed in the low pH-region of experimental studies (e.g., Kelson et al., 2017) and only found for the fastest forming hydrothermal calcites of this study and Kele et al. (2015).

6. Conclusions

The investigation of natural travertine and geothermal scale calcite from wells collected in Italy, Hungary, and Turkey suggests that DIC speciation only affects the Δ_{47} value of calcium carbonates at pH 6–8 in case of high precipitation rates ($>10^{-6}$ to 10^{-7} mol/(m^2 s)). Rapid mineral formation that does not allow for full isotopic equilibration amongst the DIC species and of DIC with water is the basis for recording disequilibrium in growing minerals. The time necessary for isotopic equilibration is strongly influenced by pH and temperature, with higher pH and lower temperature leading to much longer equilibration times. Furthermore, the isotopic difference between the DIC species is enhanced at lower temperatures and vanishes for very high temperatures. Correspondingly, at low temperatures and high pH isotopic disequilibrium effects are recorded in the forming minerals already at significantly lower growth rates. Thus, a DIC-speciation effect is more likely encountered at low temperatures and high pH values such as in certain biogenic systems and alkaline solutions, whereas low pH, high-temperature subsurface fluids should only be impacted by DIC speciation at the highest growth rates ($>10^{-6}$ to 10^{-7} mol/(m^2 s)).

This study confirms that the direct application of clumped isotope Δ_{47} values for thermometry and fluid provenance determination is also possible in the case of lower pH values, with minor (0.01‰) corrections in case of rapid mineral growth. In contrast, $\delta^{18}O$ values need to be evaluated with some caution due to potentially larger effects.

Acknowledgments
We gratefully acknowledge funding from the Qatar Carbonates and Carbon Storage Research Centre (QCCSRC), provided jointly by Qatar Petroleum, Shell, and Qatar Science & Technology Park. We thank Simon Davis for technical support, Annabel Dale and Anne-Lise Jourdan for mass spectrometer operation and calibration efforts, and the Carbonate Research group at Imperial College for fruitful discussions. We thank Enrico Capezzuoli, Memet Özkul, and Ali Gökgöz for their help during the collection of the Italian and Turkish travertine samples. József Deák and János Szanyi are acknowledged for their help in sampling calcite precipitates and thermal waters from Hungarian geothermal wells. Sándor Kele received support by the János Bolyai research scholarship of the Hungarian Academy of Sciences and the Hungarian Scientific Research Fund (OTKA 101664) and by the KH 125584 fund (NKFIH Nemzeti Kutatási, Fejlesztési és Innovációs Hivatal (Hungarian National Research, Development and Innovation Office)). We thank two anonymous reviewers for their detailed suggestions and helpful comments that helped to improve the manuscript. The data used are listed in the tables with the raw data being provided in the supporting information. The auxiliary data of Figure 5 is provided in the supporting information.

References

Affek, H. P. (2012). Clumped isotope paleothermometry: Principles, applications and challenges. In L. C. Ivany & B. M. Huber (Eds.), *Reconstructing Earth's deep-time climate—The state of the art in 2012, The Paleontological Society Papers* (Vol. 18, pp. 101–114). Boulder, CO: The Paleontological Society.

Affek, H. P. (2013). Clumped isotopic equilibrium and the rate of isotope exchange between CO_2 and water. *American Journal of Science*, *313*(4), 309–325.

Affek, H. P., Bar-Matthews, M., Ayalon, A., Matthews, A., & Eiler, J. M. (2008). Glacial/interglacial temperature variations in Soreq cave speleothems as recorded by 'clumped isotope' thermometry. *Geochimica et Cosmochimica Acta*, *72*(22), 5351–5360.

Affek, H. P., & Eiler, J. M. (2006). Abundance of mass 47 CO_2 in urban air, car exhaust and human breath. *Geochimica et Cosmochimica Acta*, *70*(1), 1–12.

Affek, H. P., Matthews, A., Ayalon, A., Bar-Matthews, M., Burstyn, Y., Zaarur, S., et al. (2014). Accounting for kinetic isotope effects in Soreq Cave (Israel) speleothems. *Geochimica et Cosmochimica Acta*, *143*, 303–318.

Al-Horani, F. A., Al-Moghrabi, S. M., & de Beer, D. (2003). The mechanism of calcification and its relation to photosynthesis and respiration in the scleractinian coral *Galaxea fascicularis*. *Marine Biology*, *142*(3), 419–426.

Andrews, J. E., Gare, S. G., & Dennis, P. F. (1997). Unusual isotopic phenomena in Welsh quarry water and carbonate crusts. *Terra Nova*, *9*(2), 67–70.

Beck, W. C., Grossman, E. L., & Morse, J. W. (2005). Experimental studies of oxygen isotope fractionation in the carbonic acid system at 15, 25 and 40°C. *Geochimica et Cosmochimica Acta*, *69*(14), 3493–3503.

Boch, R., Dietzel, M., Reichl, P., Leis, A., Baldermann, A., Mittermayr, F., et al. (2015). Rapid ikaite ($CaCO_3.6H_2O$) crystallization in a man-made river bed: Hydrogeochemical monitoring of a rarely documented mineral formation. *Applied Geochemistry*, *63*, 366–379.

Boch, R., Szanyi, J., Leis, A., Mindszenty, A., Deák, J., Kluge, T., et al. (2016). Geothermal carbonate scaling: Forensic studies applying high-resolution geochemical methods. In *Proceedings of the European geothermal congress 2016* (Pap. S-GC-111, pp. 1–10). European Geothermal Energy Council.

Bonifacie, M., Calmels, D., Eiler, J. M., Horita, J., Chaduteau, C., Vasconcelos, C., et al. (2017). Calibration of the dolomite clumped isotope thermometer from 25 to 350°C, and implications for a universal calibration for all (Ca, Mg, Fe)CO_3 carbonates. *Geochimica et Cosmochimica Acta*, *200*, 255–279.

Brand, W., Assonov, S., Coplen, T. (2010). Correction for the $_{17}$O interference in d13C measurements when analyzing CO_2 with stable isotope mass spectrometry (IUPAC technical report). *Pure and Applied Chemistry*, *82*, 1719–1733.

Chavagnac, V., Ceuleneer, G., Monnin, C., Lansac, B., Hoareau, G., & Boulart, C. (2013). Mineralogical assemblages forming at hyperalkaline warm springs hosted on ultramafic rocks: A case study from Oman and ligurian ophiolites. *Geochemistry, Geophysics, Geosystems*, *14*, 2474–2495. https://doi.org/10.1002/ggge.20146

Clark, I. D., Fontes, J. C., & Fritz, P. (1992). Stable isotope disequilibria in travertine from high pH waters: Laboratory investigations and field observations from Oman. *Geochimica et Cosmochimica Acta*, *56*(5), 2041–2050.

Clog, M., Stolper, D., & Eiler, J. M. (2015). Kinetics of CO_2(g)-H_2O(l) isotopic exchange, including mass 47 isotopologues. *Chemical Geology*, *395*, 1–10.

Cohen, A. L., & McConnaughey, T. A. (2003). Geochemical perspectives on coral mineralization. In P. M. Dove, S. Weine, & Y. DeYoreo (Eds.), *Reviews in mineralogy and geochemistry: Biomineralization* (Vol. 54, pp. 151–187). Washington, DC: Mineralogical Society of America.

Coplen, T. B. (2007). Calibration of the calcite-water oxygen-isotope geothermometer at Devils Hole, Nevada, a natural laboratory. *Geochimica et Cosmochimica Acta*, *71*(16), 3948–3957.

Daëron, M., Guo, W., Eiler, J., Genty, K., Blamart, D., Boch, R., et al. (2011). ^{13}C-^{18}O clumping in speleothems: Observations from natural caves and precipitation experiments. *Geochimica et Cosmochimica Acta*, *75*(12), 3303–3317.

Davies, A. J., & John, C. M. (2017). Reducing contamination parameters for clumped isotope analysis: The effect of lowering Porapak^{TM} Q trap temperature to below −50°C. *Rapid Communications in Mass Spectrometry*, *31*(16), 1313–1323.

Defliese, W. F., Hren, M. T., & Lohmann, K. C. (2015). Compositional and temperature effects of phosphoric acid fractionation on Δ_{47} analysis and implications for discrepant calibrations. *Chemical Geology*, *396*, 51–60.

Defliese, W. F., & Lohmann, K. C. (2015). Nonlinear mixing effects on mass-47 CO_2 clumped isotope thermometry: Patterns and implication. *Rapid Communications in Mass Spectrometry*, *29*(9), 901–909.

Demény, A., Kele, S., & Siklósy, Z. (2010). Empirical equations for the temperature dependence of calcite-water oxygen isotope fractionation from 10 to 70°C. *Rapid Communications in Mass Spectrometry*, *24*(24), 3521–3526.

Dennis, K. J., Affek, H. P., Passey, B. H., Schrag, D. P., & Eiler, J. M. (2011). Defining an absolute reference frame for 'clumped' isotope studies of CO_2. *Geochimica et Cosmochimica Acta*, *75*(22), 7117–7131.

Dennis, K. J., & Schrag, D. P. (2010). Clumped isotope thermometry of carbonatites as an indicator of diagenetic alteration. *Geochimica et Cosmochimica Acta*, *74*(14), 4110–4122.

de Nooijer, L. J., Toyofuku, T., & Kitazato, H. (2009). Foraminifera promote calcification by elevating their intracellular pH. *Proceedings of the National Academy of Sciences of the United States of America*, *106*(36), 15374–15378.

DePaolo, D. J. (2011). Surface kinetic model for isotopic and trace element fractionation during precipitation of calcite from aqueous solutions. *Geochimica et Cosmochimica Acta*, *75*(4), 1039–1056.

Dietzel, M., Tang, J., Leis, A., & Köhler, S. J. (2009). Oxygen isotopic fractionation during inorganic calcite precipitation—Effects of temperature, precipitation rate and pH. *Chemical Geology*, *268*(1–2), 107–115.

Drury, A. J., & John, C. M. (2016). Exploring the potential of clumped isotope thermometry on coccolith-rich sediments as a sea surface temperature proxy. *Geochemistry, Geophysics, Geosystems*, *17*, 4092–4104. https://doi.org/10.1002/2016GC006459

Eagle, R. A., Eiler, J. M., Tripati, A. K., Ries, J. B., Freitas, P. S., Hiebenthal, C., et al. (2013). The influence of temperature and seawater carbonate saturation state on ^{13}C-^{18}O bond ordering in bivalve mollusks. *Biogeosciences*, *10*(7), 4591–4606.

Eiler, J. M. (2011). Paleoclimate reconstruction using carbonate clumped isotope thermometry. *Quaternary Science Reviews*, *30*(25–26), 3575–3588.

Eiler, J. M. (2013). The isotopic anatomies of molecules and minerals. *Annual Review of Earth and Planetary Sciences*, *41*(1), 411–441.

Eiler, J. M., & Schauble, E. (2004). ^{18}O^{13}C^{16}O in Earth's atmosphere. *Geochimica et Cosmochimica Acta*, *68*(23), 4767–4777.

Falk, E. S., Guo, W., Paukert, A. N., Matter, J. M., Mervine, E. M., & Kelemen, P. B. (2016). Controls on the stable isotope compositions of travertine from hyperalkaline springs in Oman: Insights from clumped isotope measurements. *Geochimica et Cosmochimica Acta*, *192*, 1–28.

Fouke, B. W., Farmer, J. D., Des Marais, D. J., Pratt, L., Sturchio, N. C., Burns, P. C., et al. (2000). Depositional facies and aqueous-solid geochemistry of travertine-depositing hot springs (Angel Terrace, Mammoth hot springs, Yellowstone National Park, U.S.A.). *Journal of Sedimentary Research*, *70*(3), 565–585.

Frondini, F., Caliro, S., Cardellini, C., Chiodini, G., Morgantini, N., & Parello, F. (2008). Carbon dioxide degassing from Tuscany and Northern Latium (Italy). *Global and Planetary Change*, *61*(1–2), 89–102.

Gabitov, R. I. (2013). Growth-rate induced disequilibrium of oxygen isotopes in aragonite: An in situ study. *Chemical Geology*, *351*, 268–275.

Gabitov, R. I., Watson, E. B., & Sadekov, A. (2012). Oxygen isotope fractionation between calcite and fluid as a function of growth rate and temperature: An in-situ study. *Chemical Geology*, *306–307*, 92–102.

Garcia del Real, P., Maher, K., Kluge, T., Bird, D. K., Brown, G. E. B. Jr., & John, C. M. (2016). Clumped-isotope thermometry of magnesium carbonates in ultramafic rocks. *Geochimica et Cosmochimica Acta*, *193*, 222–250.

Ghosh, P., Adkins, J., Affek, H., Balta, B., Guo, W., Schauble, E. A., et al. (2006). ^{13}C–^{18}O bonds in carbonate minerals: A new kind of paleothermometer. *Geochimica et Cosmochimica Acta*, *70*(6), 1439–1456.

Gilfillan, S. M. V., Lollar, B. S., Holland, G., Blagburn, D., Stevens, S., Schoell, M., et al. (2009). Solubility trapping in formation water as dominant CO_2 sink in natural gas fields. *Nature*, *458*(7238), 614–618.

Gonfiantini, R., Stichler, W., & Rozanski, K. (1995). *Reference and intercomparison materials for stable isotopes of light elements* (IAEA-Tecdoc-825). Vienna, Austria: IAEA

Grauel, A.-L., Schmid, T. W., Hu, B., Bergami, C., Capotondi, L., Zhou, L., et al. (2013). Calibration and application of the 'clumped isotope' thermometer to foraminifera for high-resolution climate reconstructions. *Geochimica et Cosmochimica Acta*, *108*, 125–140.

Guo, W., Daëron, M., Niles, P., Genty, D., Kim, S. T., Vonhof, H., et al. (2008). ^{13}C-^{18}O bonds in dissolved inorganic carbon: Implications for carbonate clumped isotope thermometry. *Geochimica et Cosmochimica Acta*, *72*, A336.

Guo, W., Kim, S.-T., Yuan, J., Farquhar, J., & Passey, B. H. (2012). ^{13}C-^{18}0 bonds in dissolved inorganic carbon: Towards a better understanding of clumped isotope thermometer in biogenic carbonates. *Mineralogical Magazine*, *75*, 1791.

Guo, W., Mosenfelder, J. L., Goddard, W. A. III., & Eiler, J. M. (2009). Isotopic fractionations associated with phosphoric acid digestion of carbonate minerals: Insights from first-principles theoretical modeling and clumped isotope measurements. *Geochimica et Cosmochimica Acta*, *73*(24), 7203–7225.

Henkes, G. A., Passey, B. H., Grossman, E. L., Shenton, B. J., Perez-Huerta, A., & Yancey, T. E. (2014). Temperature limits for preservation of primary calcite clumped isotope Paleotemperatures. *Geochimica et Cosmochimica Acta*, *139*, 362–382.

Henkes, G. A., Passey, B. H., Wanamaker, A. D. Jr, Grossman, E. L., Ambrose, W. G. Jr., & Carrol, M. L. (2013). Carbonate clumped isotope compositions of modern marine mollusk and brachiopod shells. *Geochimica et Cosmochimica Acta*, *106*, 307–325.

Hesse, R. (1987). Hydrochemistry, origin and evolution of sedimentary subsurface fluids. III: Early diagenetic mineralization reactions in high sedimentation-rate basins. *Chinese Journal of Geochemistry*, *6*(2), 99–114.
Hill, P. S., Schauble, E. A., & Tripati, A. K. (2014). Theoretical constraints on the effects of pH, salinity, and temperature on clumped isotope signatures of dissolved inorganic carbon species and precipitating carbonate minerals. *Geochimica et Cosmochimica Acta*, *125*, 610–652.
Hill, P. S., Tripati, A. K., & Schauble, E. A. (2012). Predicting ^{13}C-^{18}O clumped isotope fractionation in dissolved inorganic carbon and rapidly precipitated carbonate minerals. Abstract V23B-2814 presented at the 2014 AGU Fall Meeting. San Francisco, Calif.
Huntington, K. W., Eiler, J. M., Affek, H. P., Guo, W., Bonifacie, M., Yeung, L. Y., et al. (2009). Methods and limitations of 'clumped' CO_2 isotope (Δ_{47}) analysis by gas-source isotope ratio mass spectrometry. *Journal of Mass Spectrometry*, *44*(9), 1318–1329.
Huntington, K. W., & Lechler, A. R. (2015). Carbonate clumped isotope thermometry in continental tectonics. *Tectonophysics*, *647–648*, 1–20.
John, C. M., & Bowen, D. (2016). Community software for challenging isotope analysis: First applications of 'Easotope' to clumped isotopes. *Rapid Communications in Mass Spectrometry*, *30*(21), 2285–2300.
Kele, S., Breitenbach, S. F. M., Capezzuoli, E., Nele Meckler, A., Ziegler, M., Millan, I. M., et al. (2015). Temperature dependence of oxygen- and clumped isotope fractionation in carbonates: A study of travertines and tufas in the 6–95°C temperature range. *Geochimica et Cosmochimica Acta*, *168*, 172–192.
Kele, S., Demény, A., Siklósy, Z., Németh, T., Mária, T., & Kovács, M. B. (2008). Chemical and stable isotope compositions of recent hot-water travertines and associated thermal waters, from Egerszalók, Hungary: Depositional facies and non-equilibrium fractionations. *Sedimentary Geology*, *211*(3–4), 53–72.
Kele, S., Özkul, M., Gökgöz, A., Fórizs, I., Baykara, M. O., Alçiçek, M. C., et al. (2011). Stable isotope geochemical and facies study of Pamukkale travertines: New evidences of low-temperature non-equilibrium calcite-water fractionation. *Sedimentary Geology*, *238*(1–2), 191–212.
Kelson, J. R., Huntington, K. W., Schauer, A. J., Saenger, C., & Lechler, A. R. (2017). Toward a universal carbonate clumped isotope calibration: Diverse synthesis and preparatory methods suggest a single temperature relationship. *Geochimica et Cosmochimica Acta*, *197*, 104–131.
Kharaka, Y. K., & Hanor, J. S. (2007). Deep fluids in the continents. I: Sedimentary basins. *Treatise on Geochemistry*, *5*, 499–540.
Kim, S. T., & O'Neil, J. R. (1997). Equilibrium and nonequilibrium oxygen isotope effects in synthetic carbonates. *Geochimica et Cosmochimica Acta*, *61*(16), 3461–3475.
Kluge, T., & Affek, H. P. (2012). Quantifying kinetic fractionation in Bunker Cave speleothems using Δ_{47}. *Quaternary Science Reviews*, *49*, 82–94.
Kluge, T., Affek, H. P., Dublyansky, Y., & Spötl, C. (2014). Devils Hole paleotemperatures and implications for oxygen isotope equilibrium fractionation. *Earth and Planetary Science Letters*, *400*, 251–260.
Kluge, T., Affek, H. P., Marx, T., Aeschbach-Hertig, W., Riechelmann, D. F. C., Scholz, D., et al. (2013). Reconstruction of drip-water $\delta^{18}O$ based on calcite oxygen and clumped isotopes of speleothems from Bunker Cave (Germany). *Climate of the Past*, *9*(1), 377–391.
Kluge, T., & John, C. (2015). Effects of brine chemistry and polymorphism on clumped isotopes revealed by laboratory precipitation of mono- and multiphase calcium carbonates. *Geochimica et Cosmochimica Acta*, *160*, 155–168.
Kluge, T., John, C. M., Jourdan, A.-L., Davis, S., & Crawshaw, J. (2015). Laboratory calibration of the calcium carbonate clumped isotope thermometer in the 25–250°C temperature range. *Geochimica et Cosmochimica Acta*, *157*, 213–227.
MacDonald, J., John, C. M., & Girard, J.-P. (2015). Dolomitization processes in hydrocarbon reservoirs: Insight from geothermometry using clumped isotopes. In *11th international symposium on applied isotope geochemistry (AIG)* (pp. 265–268). Amsterdam, the Netherlands: Elsevier Science BV.
McConnaughey, T. A. (2003). Sub-equilibrium oxygen-18 and carbon-13 levels in biological carbonates: Carbonate and kinetic models. *Coral Reefs*, *22*(4), 316–327.
Meckler, A. N., Adkins, J. F., Eiler, J. M., & Cobb, K. M. (2009). Constraints from clumped isotope analyses of a stalagmite on maximum tropical temperature change through the late Pleistocene. Goldschmidt Conference Abstracts, A-863. Houten, Netherlands: European Association of Geochemistry.
Meckler, A. N., Ziegler, M., Millan, M. I., Breitenbach, S. F. M., & Bernasconi, S. M. (2014). Long-term performance of the Kiel carbonate device with a new correction scheme for clumped isotope measurements. *Rapid Communications in Mass Spectrometry*, *28*(15), 1705–1715.
Metcalfe, R., Rochelle, C. A., Savage, D., & Higgo, J. W. (1994). Fluid-rock interactions during continental red bed diagenesis: Implications for theoretical models of mineralization in sedimentary basins. *Geological Society of London, Special Publications*, *78*(1), 301–324.
Mickler, P. J., Stern, L. A., & Banner, J. L. (2006). Large kinetic isotope effects in modern speleothems. *Geological Society of America Bulletin*, *118*(1–2), 65–81.
Millero, F. J., Graham, T. B., Huang, F., Bustos-Serrano, H., & Pierrot, D. (2006). Dissociation constants of carbonic acid in seawater as function of salinity and temperature. *Marine Chemistry*, *100*(1–2), 80–94.
Millero, F., Huang, F., Graham, T., & Pierrot, D. (2007). The dissociation of carbonic acid in NaCl solutions as a function of concentration and temperature. *Geochimica et Cosmochimica Acta*, *71*(1), 46–55.
Minissale, A. (2004). Origin, transport and discharge of CO_2 in central Italy. *Earth Science Reviews*, *66*(1–2), 89–141.
Mook, W. G. (2000). Environmental isotopes in the hydrological cycle: Principles and applications. In W. G. Mook (Ed.), *Introduction, theory, methods, review. IHP-V: Technical documents in hydrology* (Vol. 1, No. 39). Paris, France: UNESCO.
Müller, I., Violay, M. E. S., Storck, J.-C., Fernandez, A., van Dijk, J., Madonna, C., & Bernasconi, S. M. (2017). Clumped isotope fractionation during phosphoric acid digestion of carbonates at 70°C. *Chemical Geology*, *449*, 1–14.
Özkul, M., Kele, S., Gökgöz, A., Shen, C.-C., Jones, B., Baykara, M. O., et al. (2013). Comparison of the Quaternary travertine sites in the Denizli extensional basin based on their depositional and geochemical data. *Sedimentary Geology*, *294*, 179–204.
Passey, B. H., & Henkes, G. A. (2012). Carbonate clumped isotope bond reordering and geospeedometry. *Earth and Planetary Science Letters*, *351–352*, 223–236.
Rollion-Bard, C., Chaussidon, M., & France-Lanord, C. (2003). pH control on oxygen isotopic composition of symbiotic corals. *Earth and Planetary Science Letters*, *215*(1–2), 275–288.
Saenger, C., Affek, H. P., Felis, T., Thiagarajan, N., Lough, J. M., & Holcomb, M. (2012). Carbonate clumped isotope variability in shallow water corals: Temperature dependence and growth-related vital effects. *Geochimica et Cosmochimica Acta*, *99*, 224–242.
Schauble, E. A., Ghosh, P., & Eiler, J. M. (2006). Preferential formation of ^{13}C-^{18}O bonds in carbonate minerals, estimated using first-principle lattice dynamics. *Geochimica et Cosmochimica Acta*, *70*(10), 2510–2529.
Szanyi, J., & Kovács, B. (2010). Utilization of geothermal systems in South-East Hungary. *Geothermics*, *39*(4), 357–364.
Tang, J., Dietzel, M., Fernandez, A., Tripati, A. K., & Rosenheim, B. E. (2014). Evaluation of kinetic effects on clumped isotope fractionation (Δ_{47}) during inorganic calcite precipitation. *Geochimica et Cosmochimica Acta*, *134*, 120–136.
Thiagarajan, N., Adkins, J., & Eiler, J. M. (2011). Carbonate clumped isotope thermometry of deep-sea corals and implications for vital effects. *Geochimica et Cosmochimica Acta*, *75*(16), 4416–4425.

Tremaine, D. M., Froelich, P. N., & Wang, Y. (2011). Speleothem calcite farmed in situ: Modern calibration of ^{18}O and ^{13}C paleoclimate proxies in a continuously-monitored natural cave system. *Geochimica et Cosmochimica Acta*, *75*(17), 4929–4950.

Tripati, A. K., Eagle, R. A., Thiagarajan, N., Gagnon, A. C., Bauch, H., Halloran, P. R., et al. (2010). ^{13}C-^{18}O isotope signatures and 'clumped isotope' thermometry in foraminfera and coccoliths. *Geochimica et Cosmochimica Acta*, *74*(20), 5697–5717.

Tripati, A. K., Hill, P. S., Eagle, R. A., Mosenfelder, J. L., Tang, J., Schauble, E. A., et al. (2015). Beyond temperature: Clumped isotope signatures in dissolved inorganic carbon species and the influence of solution chemistry on carbonate mineral composition. *Geochimica et Cosmochimica Acta*, *166*, 344–371.

Uchikawa, J., & Zeebe, R. E. (2012). The effect of carbonic anhydrase on the kinetics and equilibrium of the oxygen isotope exchange in the CO_2-H_2O system: Implications for $\delta^{18}O$ vital effects in biogenic carbonates. *Geochimica et Cosmochimica Acta*, *95*, 15–34.

Usdowski, E., Michaelis, J., Böttcher, M. E., & Hoefs, J. (1991). Factors for the oxygen isotope equilibrium fractionation between aqueous and gaseous CO_2, carbonic acid, bicarbonate, carbonate, and water (19°C). *Zeitschrift Für Physikalische Chemie*, *170*, 237–249.

Venn, A., Tambutté, E., Holcomb, M., Allemand, D., & Tambutté, S. (2011). Live tissue imaging shows reef corals elevate pH under their calcifying tissue relative to seawater. *PLOS One*, *6*(5), e20013.

Wacker, U., Fiebig, J., & Schoene, B. R. (2013). Clumped isotope analysis of carbonates: Comparison of two different acid digestion techniques. *Rapid Communications in Mass Spectrometry*, *27*(14), 1631–1642.

Wainer, K., Genty, D., Blamart, D., Daëron, M., Bar-Matthews, M., Vonhof, H., et al. (2011). Speleothem record of the last 180 ka in Villars cave (SW France): Investigation of a large $\delta^{18}O$ shift between MIS6 and MIS5. *Quaternary Science Reviews*, *30*(1–2), 130–146.

Wang, Z., Schauble, E. A., & Eiler, J. M. (2004). Equilibrium thermodynamics of multiply substituted isotopologues of molecular gases. *Geochimica et Cosmochimica Acta*, *68*(23), 4779–4797.

Watkins, J., & Hunt, J. D. (2015). A process-based model for non-equilibrium clumped isotope effects in carbonates. *Earth and Planetary Science Letters*, *432*, 152–165.

Watkins, J. M., Hunt, J. D., Ryerson, F. J., & DePaolo, D. J. (2014). The influence of temperature, pH, and growth rate on the δ18O composition of inorganically precipitated calcite. *Earth and Planetary Science Letters*, *404*, 332–343.

Watkins, J. M., Nielsen, L. C., Ryerson, F. J., & DePaolo, D. J. (2013). The influence of kinetics on the oxygen isotope composition of calcium carbonate. *Earth and Planetary Science Letters*, *375*, 349–360.

Watson, E. B. (2004). A conceptual model for near-surface kinetic controls on the trace-element and stable isotope composition of abiogenic calcite crystals. *Geochimica et Cosmochimica Acta*, *68*(7), 1473–1488.

Yan, H., Liu, Z., & Sun, H. (2017). Effect of in-stream physicochemical processes on the seasonal variations in $\delta^{13}C$ and $\delta^{18}O$ values in laminated travertine deposits in a mountain stream channel. *Geochimica et Cosmochimica Acta*, *202*, 179–189.

Zaarur, S., Affek, H. P., & Brandon, M. (2013). A revised calibration of the clumped isotope Thermometer. *Earth and Planetary Science Letters*, *382*, 47–57.

Zeebe, R. E. (1999). An explanation of the effect of seawater carbonate concentration on foraminiferal oxygen isotopes. *Geochimica et Cosmochimica Acta*, *63*(13–14), 2001–2007.

Zeebe, R. E., & Wolf-Gladrow, D. (2001). CO_2 in seawater: Equilibrium, kinetics, isotopes. In *Elsevier oceanography series* (Vol. 65, 346 p.). Amsterdam, the Netherlands: Elsevier.